Proterozoic subduction-related and continental rift-zone mafic magmas from the Eastern Ghats Belt, SE India: geochemical characteristics and mantle sources

K. Vijaya Kumar[1,*], K. Rathna[1] and C. Leelanandam[2]

[1]School of Earth Sciences, SRTM University, Nanded 431 606, India
[2]House No. 12-13-205/1, Street No. 2, Tarnaka, Hyderabad 500 017, India

Understanding the origin and growth of continental crust is a fundamental problem in geological sciences. Two distinct ways in which the continental crust grows include horizontal (subduction) and vertical (plume/extension) accretions. As the mantle reservoirs in these two tectonic settings are generated and/or modified by contrasting processes, the erupted melts offer clues on the nature of these divergent mantle sources. Trace element geochemistry is a robust tool to quantitatively model the mantle sources, melting mechanisms and relative roles of mantle and crust in the petrogenesis of magmatic rocks, which ultimately lead us to unravel the origin of continental crust.

The present study portrays growth of the continental crust in the Proterozoic Eastern Ghats Belt, SE India. Mafic magmas within the Palaeoproterozoic Kondapalli–Kandra region illustrate subduction-related island arc basalt-type geochemical signatures whereas alkali basaltic magmas in the Mesoproterozoic Prakasam continental rift-zone display ocean island basalt-type characteristics. Calculated mantle sources for subduction-zone and rift-related magmas display distinctly different geochemical traits. Mesoproterozoic gabbroic magmas in the Prakasam rift-zone exhibit geochemical signatures akin to the subduction-related mafic melts. This dichotomy of continental crust produced by intra-plate processes exhibiting plate-margin signatures advocates that we possibly have overestimated the proportion of continental crust generated above subduction zones.

Keywords: Continental-rift, Eastern Ghats Belt, geochemistry, mafic magmas, mantle sources, subduction zone.

Introduction

A fundamental question concerning continental crustal growth models is whether Phanerozoic models of melt generation in the lithosphere and asthenosphere/plume are applicable to the Archaean/Proterozoic[1–3]. If so, is it possible to map the mantle reservoirs by inverting primary melt geochemistry[4,5]? Addressing this problem is paramount in as much as the two important but contrasting models of continental crustal growth which include horizontal (subduction) and vertical (plume/asthenosphere) accretions. Parameterization of geochemical models of continental crustal growth involves evaluating mantle source reservoirs and their spatio-temporal variation. For example, attending post-accretion growth of the arc/back-arc, subduction-related lithospheric sources are replaced by plume/asthenosphere upwelling and related mafic magmatism, finally culminating with the emplacement of potassic mafic melts (see ref. 6 and references therein). Thus the compositional timeline of erupted magmas in a given terrain reflects changing deep-seated mantle reservoirs. These geochemical changes in mantle source compositions and generation of new mantle reservoirs are the cornerstones of plate- and plume-tectonics.

Elucidating geochemical distinctions between the magmas derived from contrasting mantle sources has been a major geochemical focus for the past five decades. Chayes[7] was one of the early workers to recognize the geochemical distinctions between oceanic island basalt (OIB) and circum-oceanic island arc basalt (IAB). Based on distinct differences between TiO_2 and Al_2O_3 contents, he argued that the circum-oceanic basalts cannot be derived by assimilation of continental crust by OIBs. Chayes[7] suggested that the geochemical differences between the two types of basalt originated in the mantle itself. Based on experimental studies in the system MgO–SiO_2–TiO_2, MacGregor[8] suggested that the variation in TiO_2 content between OIB and IAB is controlled by depth of melting – the former with higher TiO_2 content being derived from greater depths – and ruled out separate mantle reservoirs for the two types of basalt.

With the advent of plate tectonic theory, island arc basalts are widely recognized as distinct products of subduction-related processes. The role of subducting sediment-derived fluid/melt-induced mantle metasomatism has been long realized in producing the anomalous geochemical signatures in the mantle wedge[9–11]. Generally speaking,

*For correspondence. (e-mail: vijay_kumar92@hotmail.com)

subduction fluids and associated hydrous melts are enriched in K, Rb, Th, U, Ba and LREE, and ultimately transfer them to the mantle hanging-wall. The mantle wedge may stabilize amphibole/phlogopite due to this fertilization. HFSE (high-field strength elements – Nb, Ta, Ti, P, Zr, Hf) are not readily soluble in hydrous melts and fluids, and remain in the subducted slab[12,13]. This HFSE-enriched slab may descend to greater mantle depths and finally may serve as sources of OIB magmas[11]. Accessory minerals, including ilmenite, sphene, rutile, zircon and apatite, which retain HFSE either in the slab or mantle wedge during partial melting, also play a significant role in imparting geochemical signatures characteristic of subduction-zone magmas[14–16]. However, the relative roles of partial melting, melt ascent and mantle source enrichment[17–20] responsible for the generation of these geochemical anomalies – for example, conspicuous troughs for HFSE in the primitive mantle-normalized plots – are still not fully understood. End-members for the different subduction-related mafic magmas vary from highly depleted mid-oceanic ridge basalt (MORB) to enriched OIB compositions[6,21] overprinted with subduction fluid/melt related geochemical signatures.

Similarly, modern lines of research have recognized that oceanic island basalts are largely derived from sub-lithospheric mantle sources with distinct geochemical characteristics[22–24]. Additionally, OIB-type mafic melts have also erupted on the continents, although identification of such melts is rendered difficult by plume/asthenosphere–lithosphere interaction and crustal contamination[25–29]. Favoured sources for the OIB-type magmas include: (1) subducted metasomatized oceanic lithosphere or delaminated thick continental veined lithosphere, both of which may rise as mantle plumes[30–33]; (2) metasomatically enriched asthenospheric mantle[34,35]; (3) a thermal boundary layer that was enriched by mantle plume/asthenospheric melts[36–38] and (4) enriched pockets in the sub-continental lithospheric mantle[39–42].

The southern segment of the Eastern Ghats Belt (EGB) of SE India records Palaeoproterozoic subduction-related magmatism in the Kondapalli and Kandra regions, and Mesoproterozoic rift-related magmatism within the Prakasam Alkaline Province (PAP)[43]. In the present article, we synthesize published and unpublished bulk-rock geochemical data on the mafic dykes from the Kondapalli and Kandra terrains, and PAP, representing Palaeoproterozoic (supra) subduction-zone (SSZ) and Mesoproterozoic continental rift-zone (CRZ) magmatism respectively. We interpret the compositions of the mafic dykes to evaluate the geochemical characteristics of mantle reservoirs providing the Proterozoic SSZ and CRZ magmatism.

Regional geology, tectonics, geochronology and petrography of mafic rocks

The study area lies in the southern segment of EGB, SE India (Figure 1 *a* and *b*). Based on geological and isotopic data, Dobmeier and Raith[44] subdivided the EGB into four crustal provinces. These provinces are further divided into a number of domains based on lithology, structure and metamorphic grade. The present study area falls within the Kondapalli–Ongole domain of Krishna Province. This domain experienced subduction-related arc magmatism[45–48] possibly during the period 1.85–1.70 Ga (refs 47, 49–51) followed by prolonged polyphase granulite facies metamorphism between 1.65 and 1.55 Ga (refs 52–55).

The Kondapalli Layered Complex[56], associated felsic and mafic granulites, and mafic dykes represent deeply eroded remnants of a Palaeoproterozoic (1.85–1.7 Ga) continental-margin magmatic arc[43,45–48]. Mafic dykes within the felsic granulites and metapelites show primitive mantle-derived bulk-rock geochemistries and unambiguous subduction-related characteristics[46]. Kondapalli mafic dykes exhibit porphyritic to ophitic, sub-ophitic textures with plagioclase, relict olivine, clinopyroxene and amphibole as essential phases (see Figure 1 *c*).

The Kandra Ophiolite Complex (KOC), containing well-developed sheeted dyke complex and plagiogranite, consists of new oceanic crust formed in a supra-subduction zone environment[43,51,57–60] formed at ~ 1850 Ma (ref. 51). Internal structures, lithological associations and bulk-rock compositions indicate that the KOC represents a Rocas Verdes-type continental back-arc basin[51]. The sheeted dykes are fine-grained, aphanitic to cryptocrystalline, parallel dykes with widths ranging from 4 cm to 1.25 m (refs 58 and 59). Plagioclase and Ca-amphibole (derived from clinopyroxene) are the essential phases present within KOC mafic dykes. Dykes exhibit ophitic, sub-ophitic and porphyritic textures with plagioclase and rare relict clinopyroxene phenocrysts (Figure 1 *d*). Titanite, epidote, chlorite and magnetite occur in accessory amounts.

A second major igneous event, associated with extensive tholeiitic, A-type and alkaline magmatism in the Kondapalli–Ongole domain, known as the Prakasam Alkaline Province (PAP; Figure 1 *b*) occurred between 1.35 and 1.2 Ga (refs 61–64), attending Mesoproterozoic continental rifting. Rift-zone magmatism in the PAP is represented by three geochemically distinct primary mafic magmas, alkali basaltic, gabbroic and lamprophyric dykes. This hypabyssal activity was synchronous with the emplacement of host plutons[62–67]. In the present study we discuss the bulk-rock geochemistry of only alkali basaltic dykes as they reflect the generation of a new mantle reservoir in the southern segment of the EGB. Alkali basaltic dykes exhibit porphyritic, glomeroporphyritic and panidiomorphic textures with phenocrystic assemblages of olivine–clinopyroxene ± plagioclase and olivine–plagioclase set in a groundmass of plagioclase–clinopyroxene–olivine–biotite–magnetite (Figure 1 *e*); nepheline is locally present in the groundmass. Clinopyroxene phenocrysts contain exsolved blebs of plagioclase indicating their original high-pressure crystallization[67].

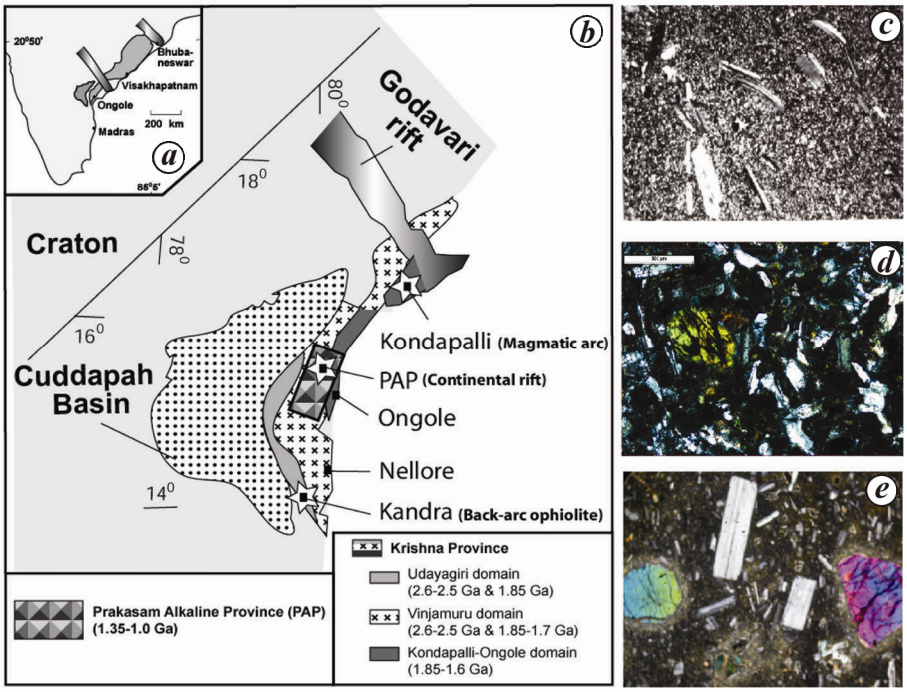

Figure 1. ***a***, Location of the Cuddapah Basin and Eastern Ghats Belt (EGB) within Peninsular India. ***b***, Generalized geological map of the southern segment of the EGB, known as Krishna Province, to the east of the Cuddapah Basin (modified after Dobmeier and Raith[44]). Mafic dykes of the present study (shown as stars) are sampled from Palaeoproterozoic subduction-related Kondapalli magmatic arc and Kandra back-arc ophiolite, and Mesoproterozoic rift-related Prakasam Alkaline Province (PAP). Note that the Mesoproterozoic rift magmatism within the PAP (shown as filled box) emplaced between the Vinjamuru and Kondapalli–Ongole domains of Krishna Province. Photomicrographs of representative mafic dykes from (***c***) Kondapalli, (***d***) Kandra and (***e***) PAP illustrate distinct textures of the rocks.

La/Nb as a geochemical proxy

Many geochemical proxies have been formulated to model the relative contributions of mantle and crustal sources involved in magma genesis. For example, Ti/Y and Zr/Y (ref. 68), Ta/Th (ref. 69), Th/Yb and Nb/Yb (refs 70 and 71), Zr/Y and Nb/Y (ref. 72), Zr/Nb and Nb/Th (ref. 73), Ce/Nb and Th/Nb (ref. 11) are some of the commonly used geochemical proxies to model physical processes. Where crustal contamination is not a major process, the La/Nb ratio is a crucial geochemical proxy for distinguishing melts derived in subduction-zone and rift-zone settings[6]. Partial melting and fractionation seem to have little influence on the La/Nb ratios[20]. The bulk-rock La/Nb ratio in oceanic basalts is 0.6–1.2; in arc basalts it is >2 and in bulk continental crust it is 2–3 (refs 74–76). Similarly, Nb/Nb* $[Nb/\sqrt{(K \times La)}]_N$, where N is MORB-normalized, is < 1 in subduction-related melts, and > 1 in asthenospheric melts. It is generally regarded that higher La/Nb ratios in the subduction magmas are due to addition of hygromagmatophile elements to the mantle sources[11].

In the present article, we have documented geochemical differences between the Kondapalli–Kandra supra subduction-zone (KK-SSZ) and the Prakasam Alkaline Province continental rift-zone (PAP-CRZ) magmas to elucidate their contrasting origins employing La/Nb and other LILE/HFSE ratios.

Geochemical characteristics of KK-SSZ and PAP-CRZ mafic magmas

Most KK-SSZ and PAP-CRZ magmas are relatively primitive (MgO = 5–20%; Table 1) with little or no crustal contamination[46,51,67]. However, some Kandra dykes exhibit evolved compositions[51] (Table 1). PAP-CRZ magmas that show geochemical signatures of plume–lithosphere interaction[67], are not considered in the present study for simplicity. In terms of average major element compositions, the KK-SSZ magmas have distinctly higher SiO_2, similar Al_2O_3, Fe_2O_3 and lower TiO_2, CaO and $Na_2O + K_2O$ contents than those of the PAP-CRZ melts. Both the groups contain high-Mg pristine mantle-derived primary melts (see MgO, Ni and Cr contents in Table 1). A higher range in MgO for subduction-related melts suggests greater degrees of fractional crystallization. However, at comparable MgO contents, the KK-SSZ magmas have higher SiO_2 contents than the PAP-CRZ magmas, as H_2O addition systematically raises the Si-saturation of the melts[77,78]. Among the trace elements,

Table 1. Average major (wt%) and trace element (ppm) compositions of the mafic dykes from the subduction-related Kondapalli and Kandra complexes and rift-related Prakasam Alkaline Province, Eastern Ghats Belt, India

	Subduction-related mafic magmas (N = 13)			Rift-related mafic magmas (N = 12)		
	Minimum	Maximum	Average	Minimum	Maximum	Average
SiO_2	46.52	55.79	51.24	43.98	48.92	45.93
TiO_2	0.36	2.88	1.46	1.13	2.52	1.83
Al_2O_3	9.92	16.75	14.11	12.93	16.67	14.62
Fe_2O_3	9.65	21.33	13.92	8.02	15.88	12.16
MnO	0.13	0.32	0.19	0.15	0.21	0.17
MgO	2.67	16.62	7.49	5.37	14.13	9.22
CaO	4.74	11.27	8.24	9.14	12.53	11.03
Na_2O	0.60	2.78	1.52	0.89	3.75	2.68
K_2O	0.15	1.92	0.58	0.62	2.07	1.28
P_2O_5	0.03	0.37	0.14	0.01	0.46	0.13
Sc	21.1	61.4	37.9	19.2	31.6	25.0
V	151	593	310	137	413	273
Cr	18.9	1713	479	105	730	509
Co	37.9	159	66.9	45.5	61.9	54.2
Ni	29.9	564	220	86.1	381	218
Cu	5.62	1154	157	36.3	199	71.3
Zn	63.5	749	160	61.7	190	120
Ga	12.8	29.7	18.5	12.6	19.8	16.2
Rb	2.27	135	21.9	3.50	67.1	24.2
Sr	25.4	524	223	342	616	452
Y	9.61	60.9	24.3	12.3	24.8	16.8
Zr	4.80	162	60.4	33.1	151	73.7
Nb	0.65	20.6	10.0	7.50	84.9	32.9
Ba	25.1	380	206	137	1152	557
Hf	0.21	3.62	1.56	0.70	3.49	1.86
Th	0.05	4.24	1.86	0.20	4.20	1.80
U	0.06	1.36	0.59	0.10	1.00	0.28
La	3.74	23.5	13.0	4.38	27.5	15.2
Ce	9.0	48.0	29.0	10.1	68.4	31.5
Pr	1.35	5.50	3.47	1.27	5.90	3.57
Nd	7.22	29.6	16.6	6.11	26.0	15.9
Sm	1.92	7.40	3.85	1.98	4.99	3.40
Eu	0.77	2.19	1.28	0.69	1.98	1.23
Gd	2.10	9.50	4.26	1.86	4.82	3.06
Tb	0.35	1.65	0.72	0.24	0.60	0.42
Dy	1.99	10.0	4.09	1.73	3.67	2.71
Ho	0.38	2.20	0.87	0.32	0.72	0.50
Er	0.97	6.54	2.40	0.95	2.04	1.30
Tm	0.10	0.90	0.33	0.13	0.32	0.18
Yb	0.70	5.74	2.14	0.78	1.90	1.16
Lu	0.10	0.89	0.33	0.12	0.24	0.18
La/Nb	2.29	5.47	3.21	0.31	0.70	0.51
Ba/Nb	4.65	178	32.7	10.3	31.3	17.7
Rb/Nb	0.44	10.8	2.31	0.25	1.22	0.75
Th/Nb	0.08	0.47	0.20	0.01	0.12	0.05
U/Nb	0.02	0.19	0.08	0.01	0.02	0.01
Y/Nb	0.82	20.8	4.19	0.25	1.64	0.68
La/Yb	2.54	19.6	7.65	4.25	22.5	13.2
Zr/Yb	3.26	54.8	28.6	29.8	129	66.3
Nb/Yb	0.44	17.2	5.58	7.28	72.5	29.1
Ti/Yb	2,132	9,935	4,936	3,849	16,827	10,282
Ti/Eu	1,796	11,810	6,889	4,945	17,464	9,905

the average compositions of compatible elements, including Ni, Cr and Co, do not show any important distinction between the KK-SSZ and PAP-CRZ magmas; however, Sc, V, Cu and Zn are clearly higher in the former. V contents in the primary basaltic liquids depend on fO_2 conditions in the mantle protolith. Higher V in the SSZ magmas may indicate elevated fO_2 conditions in their sources[79]. Large variation for Ni, Cr, Co and Sr in the KK-SSZ magmas (Table 1) is due to fractionation effects[46,51]. Average REE concentrations do not show

much variation between SSZ and CRZ melts, but the chondrite-normalized Dy/Yb ratios are variable in the former. Averages of LILE/Nb ratios are distinctly higher (by 2–7 times) in the KK-SSZ magmas than the PAP-CRZ magmas (Table 1); however, when incompatible trace elements are normalized to Yb, ratios are lower in the KK-SSZ melts than the PAP-CRZ magmas (Table 1).

Nb contents in KK-SSZ magmas range from 0.65 to 20.6 ppm and in the PAP-CRZ melts from 7.5 to 84.8 ppm (Table 1 and Figure 2). At comparable Nb contents, La abundances in the KK-SSZ mafic magmas are 2–3 times higher than the PAP-CRZ melts. The KK-SSZ magmas have La/Nb > 1 (2.3–5.5) and PAP-CRZ melts have La/Nb < 1 (0.31–0.70; Figure 2). Th/Nb and U/Nb values in general are higher in subduction-related magmas than in the continental rift-zone magmas[23], as reflected in the Proterozoic KK-SSZ and PAP-CRZ mafic magmas of the EGB (Figure 3). Enrichment of Th and U over Nb in SSZ magmas is not only controlled by source composition but also by the partial melting processes. Mantle minerals have lower distribution coefficients for Th and U than for Nb. As a result, Th/Nb and U/Nb ratios in the melt are greater than those in the sources.

Representative chondrite-normalized REE patterns of KK-SSZ and PAP-CRZ melts are depicted in Figure 4. The former shows two distinct REE patterns in terms of La/Yb slopes. Melts with steeper slopes were presumably formed by lower degrees of melting, whereas near flatter ones were generated by moderate degrees of melting. However, mantle sources for both these melts with variable La/Yb ratios seem to be uniform as indicated by their La/Nb, Th/Nb and U/Nb ratios (Figures 2 and 3). Negative Eu anomalies in some of the SSZ melts are due to fractionation effects. The PAP alkali basaltic magmas show uniform LREE fractionated patterns without any prominent anomalies for Eu. $(Dy/Yb)_N$ ratios in both SSZ and CRZ melts suggest that they were derived within the garnet–spinel lherzolite stability field. Derivation from the garnet-only stability field produces much steeper $(Dy/Yb)_N$ slopes[80]. Ti/Eu, which is considered to be independent of melting, is higher in the CRZ than the SSZ magmas. PAP-CRZ melts evidently formed by lower degrees of melting[67], but KK-SSZ melts seem to have been derived by low to moderate degrees of melting of mantle sources (Figure 4).

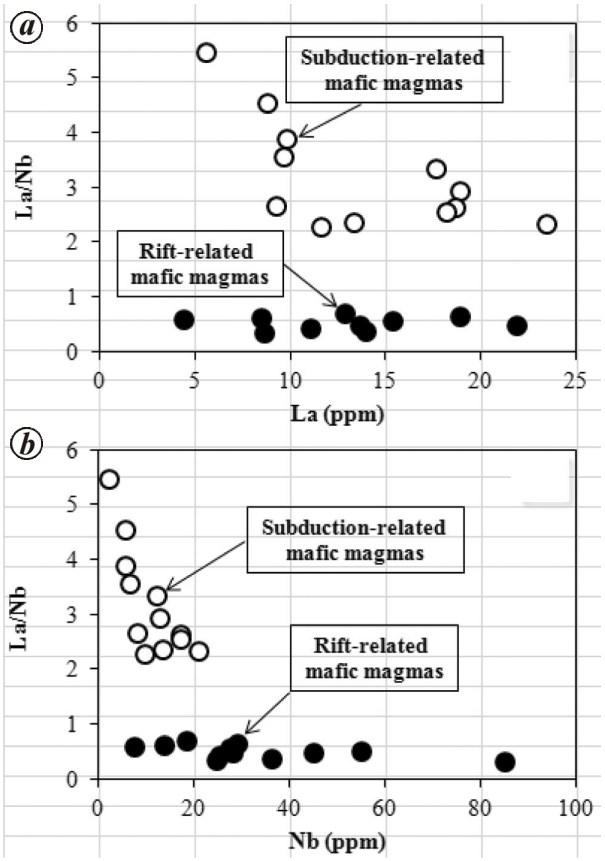

Figure 2. (*a*) La versus La/Nb and (*b*) Nb versus La/Nb variation in the Kondapalli and Kandra suprasubduction-related (KK-SSZ), and the PAP continental-rift (PAP-CRZ) mafic magmas from the EGB. Distinctly higher La/Nb ratio for the subduction-related magmas is conspicuous. See text for discussion.

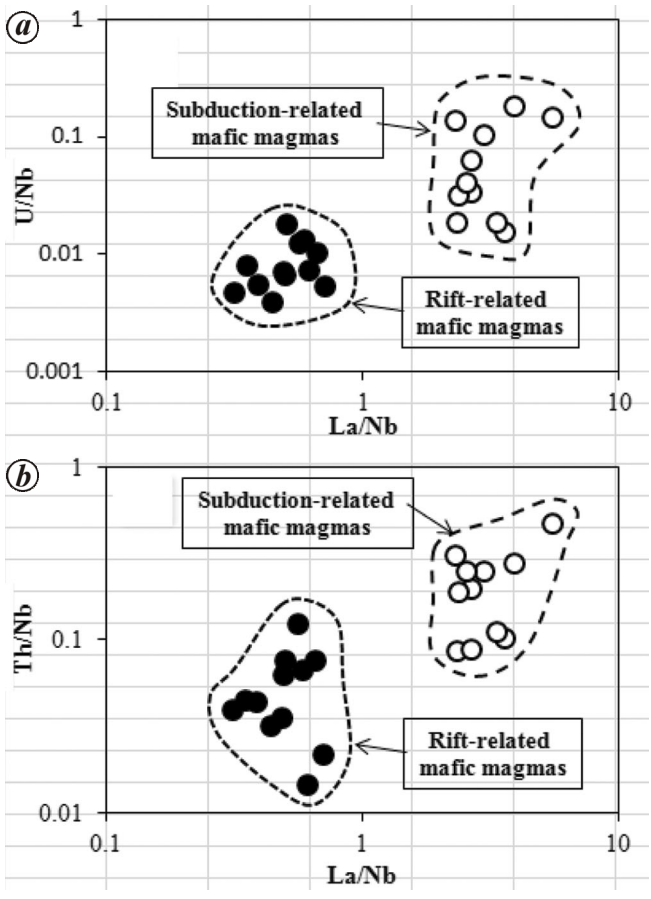

Figure 3. (*a*) La/Nb versus U/Nb and (*b*) La/Nb versus Th/Nb variation in the KK-SSZ and PAP-CRZ mafic magmas of the EGB. Note that the Palaeoproterozoic subduction-related magmas of the EGB have distinctly higher LILE/HFSE elemental ratios than the Mesoproterozoic rift-related magmas. See text for discussion.

Mantle sources to KK-SSZ and PAP-CRZ mafic magmas

Geochemical characteristics of the mantle sources and their generation are discussed in this section. All subduction-related basalts are essentially derived from MORB–OIB mantle sources influenced by fluids and melts released from the subducting lithosphere[6,21,81,82]. Thompson *et al.*[6] suggested that low-K island-arc tholeiites are hydrous analogues of MORB, whereas calc-alkaline tholeiites are counterparts of OIB tholeiites. Plank[21] modelled the geochemical anomalies of subduction-zone melts in terms of mixing between mantle melts and subducting sediments. The KK-SSZ magmas show a progressive variation in Sm/La and Th/La ratios from an initial enriched mid-ocean ridge basalt (EMORB) bulk-rock chemistry towards global subducting sediment (GLOSS)[83] composition (Figure 5). Such a variation is interpreted in terms of a subduction overprint on original oceanic mantle sources, as is typical of supra-subduction zone environments[21,84]. KK-SSZ magmas are similar to the geochemical variation represented by present-day Aleutians and Java subduction-related magmas (Figure 5). Some of the KK-SSZ magmas have Sm/La and Th/La compositions similar to that of the OIB (Figure 5). It is important to note that the OIB-type mantle replenishes the source regions of arc magmatism as the melts are driven away from mantle wedge[11]. Geochemical characteristics of KK-SSZ magmas clearly indicate the important role of subducted sediments in the geochemical modification of hanging-wall mantle sources in the supra-subduction-zone[84].

La/Nb and La/Yb values demonstrate IAB-type characteristics for KK-SSZ magmas, whereas OIB-type geochemical signatures are evident for PAP-CRZ alkali basaltic melts. The role of crustal contamination in the production of negative anomalies for HFSE in KK-SSZ mafic magmas was keenly debated and negated by earlier studies[43,67]. All KK-SSZ magmas, irrespective of their MgO contents, contain lower Nb abundances, suggesting a modest role for crust in the generation of troughs for HFSE in primitive mantle-normalized diagrams. Geochemical signatures of KK-SSZ magmas can be explained by 20–30% mixing between melts of EMORB composition and GLOSS (Figure 6 *a*). From this plot it is evident that the La/Nb ratio slightly decreases by partial melting in rift settings, as illustrated by plots of EMORB, OIB and PAP mafic melts lying to the left of primitive mantle, or the source has a lower La/Nb than the primitive mantle. La/Yb ratio is sensitive to the degree of melting, with higher values for low-degree melts. Similar geochemical traits for the OIB and PAP magmas (Figure 6 *a*) suggest low-degree melting of the mantle sources for the latter. Average La/Yb ratios of PAP-CRZ magmas are

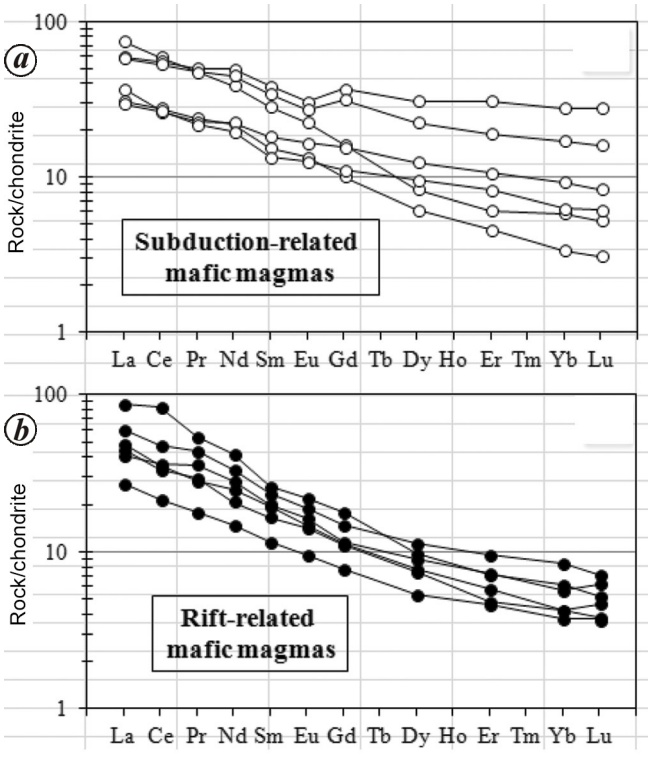

Figure 4. Chondrite-normalized REE patterns for the (***a***) KK-SSZ and (***b***) PAP-CRZ magmas of the EGB. The subduction-related mafic magmas show steep to moderate fractionated REE patterns with none to gentle negative Eu anomalies whereas the rift-related alkali basaltic magmas exhibit uniform steeply fractionated REE patterns without Eu anomalies. Normalizing values are after Hanson[80]. See text for discussion.

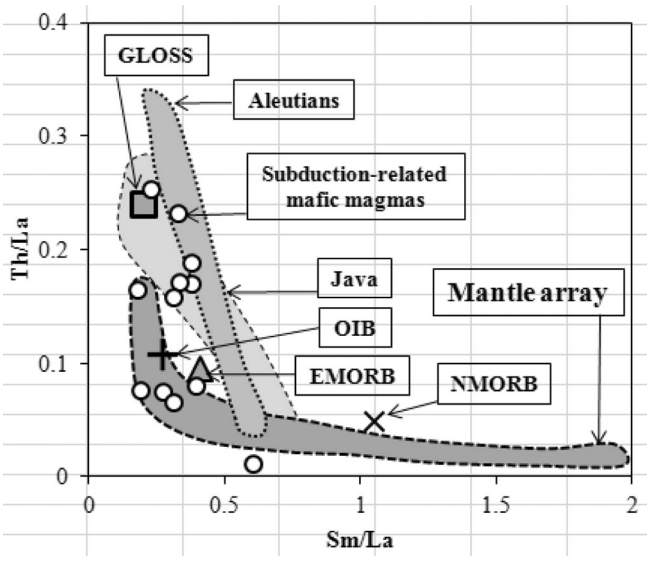

Figure 5. Sm/La versus Th/La variation in the KK-SSZ magmas. Subduction-related magmas from Aleutians and Java are shown for comparison. Data sources: Refs 21, 83 and 87. Compositions of EMORB (enriched mid-oceanic ridge basalt), OIB (Ocean Island Basalt), NMORB (normal mid-oceanic ridge basalt), GLOSS (Global Subducting Sediment) are shown for comparison. The subduction-zone magmas from the EGB can be considered as products of EMORB and GLOSS mixing. See text for discussion.

slightly higher than those in the KK-SSZ magmas, indicating that the latter were formed by relatively higher degrees of melting.

Similar results are obtained using Nb/Yb ratios (Figure 6 *b*), which are distinct for IAB- and OIB-type sources; these ratios are especially controlled by Nb contents in the sources and depths of melting. Relatively low-degree melts among the SSZ magmas exclusively come from the Kondapalli magmatic arc, whereas moderate degree melts come from both the Kondapalli and Kandra complexes. It is well established that melting would be deeper beneath thick magmatic arcs, whereas it is shallower and involves greater degree of melting beneath back-arcs[85,86]. Nb/Yb is an order of magnitude higher in the OIB-type PAP-CRZ melts than the IAB-type KK-SSZ melts. On the basis of La/Nb and Nb/Yb ratios, it is evident that Nb is more incompatible than La during melting beneath continental rifts. The KK-SSZ magma composition can be explained by mixing between EMORB and GLOSS (Figure 6 *b*).

For calculating the mantle sources of the KK-SSZ magmas, we formulated two independent geochemical approaches. In the first, we inverted the trace element chemistry of the EMORB[87], presuming $F = 10\%$ and considering a spinel lherzolite source (Table 2) for data on source mineralogy and partition coefficients) and using non-modal batch melting equation[88]. Our choice of EMORB is based on the fact that the KK-SSZ magmas show a progressive variation in Sm/La and Th/La ratios from an initial EMORB bulk-rock chemistry towards GLOSS. For the choice of other parameters including degrees of melting, mantle mineralogy and type of melting; see ref. 5. To the mantle source for the EMORB so calculated, we added GLOSS in the proportion 0.98 : 0.02. The mantle source generated by this bulk mixing is shown in Figure 7. In the second approach, a primitive melt (MgO = 16.6 wt%; Ni = 564 ppm) in the KK-SSZ magmas was inverted to calculate source composition with

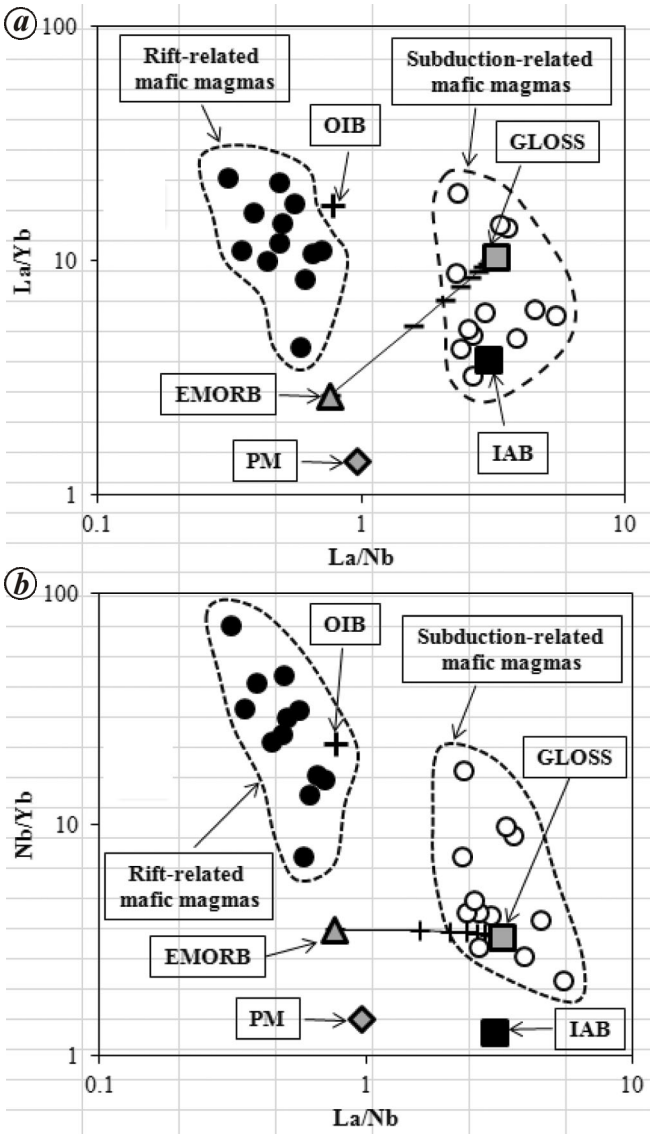

Figure 6. (***a***) La/Nb versus La/Yb and (***b***) La/Nb versus Nb/Yb variation in the KK-SSZ and PAP-CRZ mafic magmas of the EGB. Compositions of PM (primitive mantle), EMORB, OIB, IAB (Island Arc Basalt) and GLOSS are shown for comparison. Mixing between EMORB and GLOSS explains the chemistry of subduction-related magmas of the Kondapalli and Kandra areas. Each tick mark on the mixing curve indicates 10% mixing. The PAP rift-zone magmas have compositions similar to that of the OIB. See text for discussion.

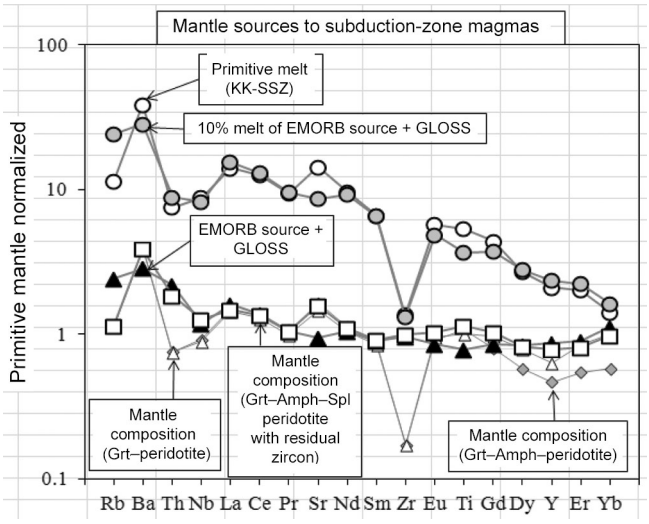

Figure 7. Primitive mantle-normalized plot showing the calculated mantle source and melt incompatible element abundances for the genesis of subduction-related mafic magmas from Kondapalli and Kandra areas. Two independent geochemical approaches are formulated for calculating the mantle sources for the KK-SSZ magmas. In the first approach we inverted the trace element chemistry of the EMORB[87] to calculate the mantle source composition. To this we added GLOSS in the proportion 0.98 : 0.02. In the second approach, primary melt to the KK-SSZ magmas was inverted to calculate source composition with or without zircon in the residue. Melt produced by 10% melting of the EMORB source + GLOSS mixture in the garnet–spinel stability field with residual zircon is similar to the primitive melt to the KK-SSZ magmatism. See text for discussion. Data sources: refs 19 and 87 (EMORB and primitive mantle) and refs 19, 109, 110 (partition coefficients).

Table 2. Details of melting equation, mantle source mineralogy, melting proportions and mineral/melt partition coefficients used in calculations

A. Equation used in the calculations

(i) Non-modal batch melting[88]:

$$\frac{C_i^l}{C_i^0} = \frac{1}{[D_i^0 + F(1 - P_i)]},$$

where C_i^l is the concentration of element i in the liquid, C_i^0 the initial concentration of element i in the original source, D_i^0 the initial solid bulk distribution coefficient ($\sum X_i Kd_i$), P_i the weighted distribution coefficient of the liquid and F is the degree of melting.

B. Source mineralogy and melting proportions (compiled from the literature)

Phase proportion	Grt–Perid	Grt–Spl–Perid	Grt–Amph–Perid	Grt–Phl–Perid	Grt–Spl–Amph–Perid
Ol	0.60	0.55	0.60	0.60	0.55
Opx	0.21	0.22	0.21	0.21	0.18
Cpx	0.08	0.15	0.08	0.08	0.08
Spl	0.00	0.02	0.00	0.00	0.04
Grt	0.11	0.06	0.06	0.07	0.10
Amph	0.00	0.00	0.05	0.00	0.05
Phl	0.00	0.00	0.00	0.04	0.00
Melting proportions					
Ol	–0.10	–0.10	–0.10	–0.10	–0.10
Opx	0.25	0.25	0.25	0.25	0.25
Cpx	0.61	0.61	0.61	0.61	0.51
Spl	0.00	0.04	0.00	0.00	0.10
Grt	0.24	0.20	0.24	0.24	0.24
Amph	0.00	0.00	0.00	0.00	0.00
Phl	0.00	0.00	0.00	0.00	0.00

C. Mineral/melt partition coefficients (compiled from the literature)

	Ol	Opx	Cpx	Spl	Grt	Amph	Phl	Zir*
Rb	0.0003	0.0002	0.0004	0.0001	0.0002	0.023	1.7	0.006
Ba	5E-06	6E-06	0.0003	0.0001	0.00007	0.01	1.5	0.004
Th	7E-06	0.00002	0.0021	0.0001	0.0021	0.001	0.1	145
Nb	0.00005	0.003	0.0089	0.01	0.01	0.08	0.14	40
La	0.0002	0.0031	0.054	0.00002	0.0007	0.075	0.003	0.05
Ce	0.00007	0.0021	0.086	0.00003	0.0026	0.11	0.021	0.99
Pr	0.0003	0.0026	0.15	0.0001	0.005	0.15	0.0053	0.3
Sr	0.00004	0.0007	0.091	0.0002	0.0007	0.27	0.044	0.034
Nd	0.0003	0.0023	0.19	0.0002	0.027	0.23	0.0063	0.5
Sm	0.0009	0.0037	0.27	0.0004	0.22	0.32	0.0059	3.56
Zr	0.001	0.012	0.26	0.07	0.2	0.25	0.13	600
Eu	0.0005	0.009	0.43	0.0006	0.61	0.52	0.031	4
Ti	0.015	0.086	0.4	0.15	0.6	0.95	0.98	3.15
Gd	0.0011	0.0065	0.44	0.0009	1.2	0.53	0.0082	13
Dy	0.0027	0.011	0.44	0.0015	2	0.5	0.026	22.45
Y	0.0082	0.015	0.47	0.002	3	0.54	0.03	10
Er	0.0109	0.021	0.39	0.003	3.3	0.46	0.03	19
Yb	0.024	0.038	0.43	0.0045	6.4	0.5	0.03	58

*Calculated from the partition of trace elements between zircon and basaltic melts of Kondapalli–Kandra.
Ol, Olivine; Opx, Orthopyroxene; Cpx, Clinopyroxene; Spl, Spinel; Grt, Garnet; Amph, Amphibole; Phl, Phlogopite; Zir, Zircon.

or without zircon in the residue. Although forward modelling, adopted here presents a variety of possibilities depending on the choice of model source, degree of melting and type of melting, close geochemical similarity between sources estimated from these two independent approaches gives us a sense of confidence in the calculations. Mantle source calculated from both the approaches shows troughs for HFSE elements, especially prominent for Th, Nb, Zr, Ti and Y. Proposed mechanisms for the HFSE depletion in arc magmas include: (1) their retention in subducting slab and relative enrichment of LILE by addition of slab-derived fluids and melts to the mantle wedge[86,89–92]; (2) inheritance from subducting sediment through bulk assimilation[21]; (3) development of HFSE

depletion during melting of mantle wedge[19]; (4) mantle-melt reaction during ascent[18] and (5) existence of shallow HFSE-depleted mantle reservoirs due to earlier melt removal, i.e. original Nb depletion in mantle sources[93,94]. Absolute abundances of Nb, Zr and Ti in subduction-zone mantle sources may or may not be different from the Normal MORB (NMORB) or EMORB mantle sources[20,95], depending on the material added to the mantle wedge. If only fluids are added, then there will be exclusive addition of LILE to mantle sources beneath subduction-zones, thereby producing sources with higher LILE/HFSE ratios than the NMORB or EMORB sources. If slab-derived melts or bulk-sediment assimilates are the enriching materials, this may lead to LILE enrichment as well as HFSE depletion in the subduction-zone sources. It is likely that HFSE depletions in subduction-zone melts may be further enhanced by stabilization of minerals with higher partition coefficients for HFSE such as amphibole, zircon and rutile/ilmenite during partial melting of the mantle wedge.

For the KK-SSZ magmas, we suggest that depletion in the HFSE in the mantle source took place prior to the melting due to addition of LREE-rich slab flux; retention of minor phases during partial melting further amplified the anomalies. A mantle source calculated with zircon in the residue matches with that calculated by mixing of an EMORB source with GLOSS (Figure 7). Although we have modelled considering zircon as a residual phase in the mantle wedge, it is more likely that it was a residual phase during slab melting. It has been suggested that Th/La ratio in the basaltic melts is independent of the melting process and reflects the contribution from subducting sediments[21]. However, if zircon is a residual phase, as suggested in the present study, then Th/La ratio is controlled by sediment contribution as well as the melting process (Figure 7). Melt produced by 10% melting of the EMORB source + GLOSS mixture is similar to the primary melt to the KK-SSZ magmatism (Figure 7). Minor deviations for Sr and Ti, both in the calculated mantle source and partial melt, suggest possible involvement of apatite and ilmenite in the melting process. Characteristic geochemical signatures for the arc magmas, as is evident from the calculations, are generated at the mantle sources themselves.

OIB-type mantle sources are generated by recycling of subducted, metasomatized oceanic lithosphere or delaminated thick continental veined lithosphere into asthenospheric mantle[96,97]. The OIB-type signatures for the continental alkaline basalts involve prior depletion and later enrichment of the mantle sources – a two-stage mantle model[97]. We have calculated incompatible elemental abundances of a mantle source for PAP alkali basalts using this two-stage model[97] (Figure 8). In stage one, a basaltic melt is extracted from the DMM (depleted MORB mantle) sources in the garnet–spinel stability field; in stage two, this depleted source is enriched by low-degree partial melt that was also derived from a DMM source but within the garnet stability field. Details of DMM composition, proportions of melt extraction and addition are given in the caption to Figure 8. We have also inverted the primary melt (MgO = 14.1 wt%; Ni = 381 ppm) incompatible element chemistry to calculate the mantle source composition, on similar lines that we have estimated the sources for KK-SSZ magmas. Details of our calculations are given in the caption to Figure 8. The computed incompatible element abundances from the primary melt inversion and the two-stage model of mantle source to PAP alkali basalt dykes are similar to that of the source for continental alkali basalts[97]. Such a pre-extraction of magmas is reflected by convex downward pattern for the Zr–Yb segment in the primitive mantle-normalized abundances of the sources. Five per cent melt of the two-stage-mantle source generated within the garnet–spinel stability field explains the trace element characteristics of the PAP-CRZ magmas (Figure 8).

Growth of new continental crust or recycling of old continental crust?

Assessment of relative proportion of created and inherited geochemical signatures along convergent plate margins is

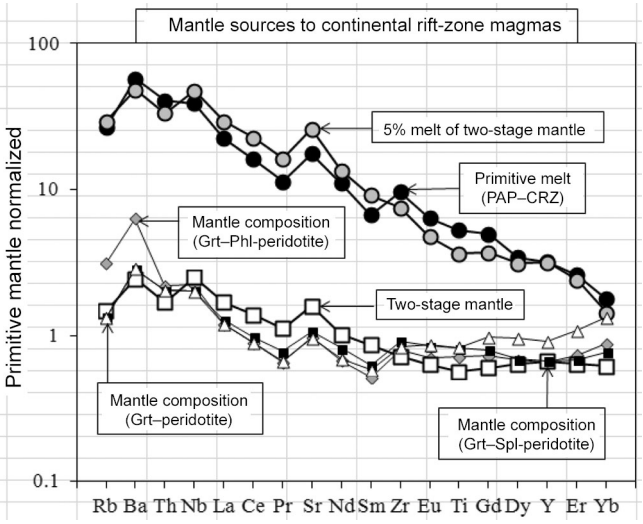

Figure 8. Primitive mantle-normalized plot showing the calculated mantle source and melt incompatible element abundances for the genesis of rift-related PAP alkali basaltic magmas. Calculation of incompatible element abundances of mantle sources for the PAP alkali basaltic magmas involves extraction of 11% basaltic melt from a DMM (depleted MORB mantle) source within the garnet–spinel stability field followed by enrichment of this depleted source by 8% of a melt formed by 0.4% melting of the DMM source in the garnet stability field. Pre-extraction of basaltic magma is reflected in the convex-downward pattern for the elements Zr to Yb in the normalized plots for alkali basalt mantle sources. Five per cent melting of this metasomatized DMM source within garnet–spinel stability field produces a melt with concentrations similar to the PAP primitive alkali basaltic magma. Melting in garnet-only stability field produces much stronger fractionation trends. Non-modal batch melting equation[88] is used in all the calculations. Data sources: Ref. 19 (primitive mantle), ref. 111 (DMM) and refs 19, 109, 110 (partition coefficients).

vital to estimate whether the continental crust is recycled or a new sialic crust is created. If the geochemical anomalies are inherited from subducting sediments alone, it indicates that the continental crust is being recycled. However, if the geochemical signatures are created at the subduction zones by mantle-based magmatic processes, then it can be interpreted as growth of new continental crust. For example, Nb anomalies can be created by sediment melting in the subducting slab[92,98] or can be simply inherited from the sediments[21]. Distinction between created and inherited HFSE anomalies is imperative in addressing whether new continental crust is generated with time or the old crust is being simply recycled.

It is evident from the estimated source compositions for KK-SSZ magmatism that zircon was present in the residue during partial melting either of the subducting slab or the mantle wedge after mixing with the slab-derived component (Figure 7). Residual phases during super-solidus experiments on the slab sediments include garnet, rutile and zircon[99], which indicate that HFSE and HREE can be retained in the slab residue even during high degrees of melting under H_2O-saturated conditions. However, retention of the minor phases during mantle wedge melting is rather difficult due to relatively high temperatures of melting (1000–1100°C). If these minor phases are indeed retained in the residue even at such conditions, then they may have been present as small inclusions in major restite phases. Such a mechanism would explain the Zr-poor and Zr-rich lamproite magmas in the Cuddapah Basin[100]. From estimated mantle source compositions, it is evident that simple mixing of EMORB sources and GLOSS does not explain primitive mantle-normalized elemental patterns when all the incompatible elements are considered and calls for unequivocal involvement of magmatic processes in the generation of subduction-related geochemical signatures. By implication, the continental crust in the Kondapalli–Kandra region is newly generated and does not record recycled older continental crust. Recently generated zircon U–Pb age data record only Palaeoproterozoic ages and do not record any Archaean crust in the Kondapalli–Kandra protoliths, including felsic rocks[101] (Vijaya Kumar *et al.*, unpublished data).

Long-term geochemical memories of continental lithosphere

Vijaya Kumar and Leelanandam[43] proposed that the growth of continental crust along the SE margin of India was created by subduction-related processes. The present study confirms the proposition that new mantle reservoirs were generated during the Palaeoproterozoic by subduction, and that the Kondapalli and Kandra mafic magmas are a crustal expression of these geochemically distinct mantle sources. Subduction-zone magmas of the Kondapalli region come from a magmatic arc, whereas the Kandra magmas represent Rocas–Verdes-type continental back-arc ophiolite[51]. However, both the magma suites are geochemically similar (Figure 9), suggesting the existence of a regional mantle reservoir influenced by subduction processes. With increasing arc proximity, the back-arc basalts display subduction-dominated signatures[102,103]. Prior to subduction, the mantle had a composition similar to sources of the present-day EMORB. Melting of EMORB-type mantle sources overprinted by subduction processes on a regional scale explains the magma genesis and Palaeoproterozoic crustal growth along the SE margin of India.

The geochemistry of PAP gabbroic magmas indicates a subduction influence in their source regions, though they were emplaced in an extensional regime during Mesoproterozoic continental rifting[67] (Figure 9). This contradiction can be reconciled if the source regions had retained subduction signatures that were acquired in a previous tectonic environment. For example, Dudás[104] argued that 'arc-signatures' shown by 'rift-related' Eocene magmatism of North America reflect ancient lithospheric enrichment events. The former presence of palaeo-subduction-related lithospheric mantle beneath the central North China craton was indicated by the bulk-rock geochemistry of Cretaceous gabbroic rocks of the Taihang Mountains[105]. Long geochemical memories of subcontinental lithospheric mantle were also proposed by Goodenough *et al.*[42] based on their studies of the Mesoproterozoic Gardar magmas. They demonstrated that the lithospheric mantle acquired subduction-related geochemical signatures around 1.8 Ga, but that this enriched

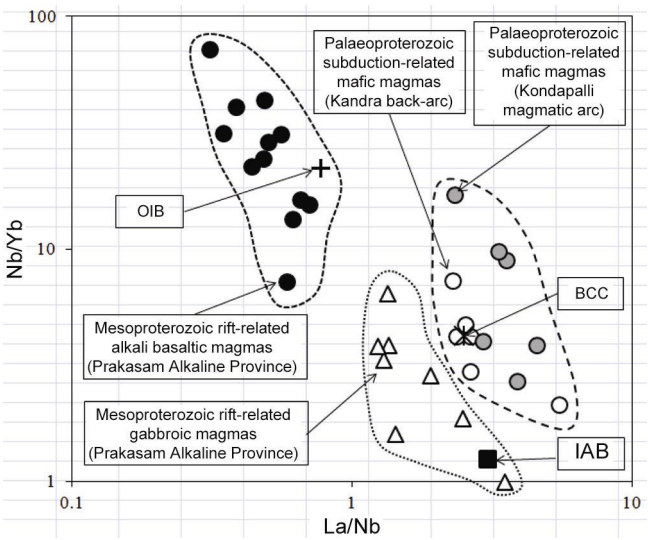

Figure 9. La/Nb versus Nb/Yb variation in the subduction-related mafic magmas from Palaeoproterozoic Kondapalli and Kandra complexes and continental-rift related alkali basaltic and gabbroic magmas from the Mesoproterozoic PAP of the EGB. Compositions of OIB, IAB and BCC (bulk continental crust) are shown for comparison. Note that the Mesoproterozoic rift-zone gabbroic magmas show geochemical signatures akin to subduction environments. See text for discussion.

mantle was melted and removed during 1.3 Ga Gardar rifting. Lithospheric mantle beneath PAP seems to have been enriched by subduction-related events around 1.8–1.6 Ga, which produced the Kondapalli magmatic arc and Kandra back-arc[43,47,51,106]. Subsequent to this enrichment, the lithosphere mantle was quiescent for ~400 Myr and then underwent melting at the time of continental rifting ~1.35 Ga.

The presence of arc-related magmas in a rift-setting further indicates that the generation of mantle sources and their subsequent melting could be two fundamentally independent and clearly unrelated events separated by a large time gap. Subduction-modified lithospheric mantle may provide a source for subsequent CRZ magmatism either immediately after subduction or even after a prolonged time gap, as demonstrated by Johnson *et al.*[107] and Goodenough *et al.*[42]. Understanding the long-term retention of subduction-related signatures by the continental lithosphere is imperative to evaluate the sites of generation of sialic crust. Average bulk continental crust (BCC) has La/Nb ratios similar to those of the Palaeoproterozoic Kondapalli–Kandra subduction-related magmas (Figure 9). The geochemical similarity between BCC and arc basalts prompted many workers to suggest that the continental crust was generated at subduction zones. Based on geochemical characteristics of arc basalts and bulk continental crust, researchers[75,76,108] estimated that 85–95% of the continental crust has been generated at subduction zones. The PAP gabbroic dykes were formed during Mesoproterozoic continental rifting, but show distinct subduction-related signatures. An implication of this observation is that continental crust can be produced by intraplate processes with plate-margin signatures. A larger implication is that unless we recognize the proportions of crust produced in intraplate settings with subduction signatures, our estimate of continental crust generation at subduction zones will be an overestimate.

Conclusions

Our study suggests the creation of distinct mantle sources during Palaeoproterozoic and Mesoproterozoic times along the SE margin of India. Palaeoproterozoic crustal growth was by subduction-related processes, whereas the Mesoproterozoic crustal growth was controlled by addition of mafic melts derived from plume-like and continental lithosphere sources in a rift setting. The study further suggests that both melting process and mantle source composition are significant in the generation of geochemical characteristics diagnostic of arc basalts. It is not possible to create the melts with distinct anomalies for HFSE solely based on melting mechanism of a primitive mantle with or without amphibole in the residue. Troughs for Nb, Zr and Ti are generated at the mantle sources themselves, either by addition of slab-derived partial melts or bulk assimilation of a GLOSS-like composition. We have modelled mantle sources using a bulk assimilation technique. Melting of these modified mantle sources generates basaltic melts with characteristic subduction-related magmatic signatures. Geochemical parameters suggest that the KK-SSZ magmas were generated by mixing of the mantle wedge and global subducting sediments. Pre-subduction chemistry of the mantle sources is close to the source of EMORB. Troughs in HFSE in the mantle source were developed prior to melting and were connected to LREE-rich slab flux; accessory mineral saturation during partial melting of either the slab sediments or metasomatized mantle source further amplified the negative anomalies for HFSE. Sources for PAP-CRZ magmas were produced by a two-stage mechanism: extraction of basaltic magma from DMM sources in the first stage followed by addition of small-degree partial melt also derived from DMM sources, in the second stage. Low-degree partial melting of these hybrid sources explains the geochemical characteristics of PAP-CRZ magmas. Mesoproterozoic rift-related gabbroic melts exhibit geochemical signatures akin to subduction-related magmas. We interpreted this dichotomy of rift-zone magmas showing arc signatures in terms of the Mesoproterozoic mantle retaining subduction characteristics developed during the Palaeoproterozoic. Continental lithosphere with subduction memories was melted after a gap of 400 Myr. Production of sialic crust by an intraplate process with plate-margin signatures suggests that we may overestimate the proportion of continental crust generated at subduction zones. Voluminous Palaeoproterozoic subduction-related and Mesoproterozoic rift-related magmatism within the EGB provides strong evidence for evolving mantle reservoirs and lithosphere characteristics in space and time.

1. Krogstad, E. J., Balakrishnan, S., Mukhopadhyay, D. K., Rajamani, V. and Hanson, G. N., Plate tectonics 2.5 billion years ago: evidence at Kolar, South India. *Science*, 1989, **243**, 1337–1340.
2. Stern, R. J., Evidence from ophiolites, blueschists and ultrahigh-pressure metamorphic terranes that the modern episode of subduction tectonics began in the Neoproterozoic. *Geology*, 2005, **33**, 557–560.
3. Brown, M., Duality of thermal regimes is the distinctive characteristic of plate tectonics since Neoarchean. *Geology*, 2006, **34**, 961–964.
4. Rajamani, V., Shivkumar, K., Hanson, G. N. and Shirey, S. B., Geochemistry and petrogenesis of amphibolites, Kolar schist belt, South India: evidence for komatiitic magma derived by low percentages of melting of the mantle. *J. Petrol.*, 1985, **26**, 92–123.
5. Vijaya Kumar, K., Reddy, M. N. and Leelanandam, C., Dynamic melting of the Precambrian mantle: evidences from rare earth elements of the amphibolites from the Nellore–Khammam schist belt, South India. *Contrib. Mineral. Petrol.*, 2006, **152**, 243–256.
6. Thompson, R. N., Morrison, M. A., Hendry, G. L. and Parry, S. J., An assessment of the relative roles of crust and mantle in magma genesis: an element approach. *Philos. Trans. R. Soc. London, Ser.*, 1984, **310**, 549–590.

7. Chayes, F., Titania and alumina content of oceanic and circum-oceanic basalt. *Mineral. Mag*., 1965, **34**, 126–131.
8. MacGregor, T. D., The system $MgO–SiO_2–TiO_2$ and its bearing on the distribution of TiO_2 in basalts. *Am. J. Sci., Schairer Vol.*, 1969, **267A**, 342–363.
9. Hole, M. J., Saunders, A. J., Marriner, G. F. and Tarney, J., Subduction of pelagic sediments; implications for the origin of Ce-anomalous basalts from the Mariana islands. *J. Geol. Soc. London*, 1984, **141**, 453–472.
10. Tera, F., Brown, L., Morris, J., Sacks, I. S., Klein, J. and Middleton, R., Sediment incorporation in island-arc magmas: inferences from ^{10}Be. *Geochim. Cosmochim. Acta*, 1986, **50**, 535–550.
11. Saunders, A. D., Norry, M. J. and Tarney, J., Fluid influence on the trace element compositions of subduction zone magmas. *Philos. Trans. R. Soc. London*, *Ser. A*, 1991, **335**, 377–392.
12. Brenan, J. M., Shaw, H. F., Ryerson, F. J. and Phinney, D. L., Mineral–aqueous fluid partitioning of trace elements at 900°C and 2.0 GPa: constraints on the trace element chemistry of mantle and deep crustal fluids. *Geochim. Cosmochim. Acta*, 1995, **59**, 3331–3350.
13. Kessel, R., Schmidt, M. W., Ulmer, P. and Pettke, T., Trace element signature of subduction-zone fluids, melts and supercritical liquids at 120–180 km depth. *Nature*, 2005, **437**, 724–727.
14. Ayers, J. C. and Watson, E. B., Solubility of apatite, monazite, zircon and rutile in supercritical aqueous fluids with implications for subduction zone geochemistry. *Philos. Trans. R. Soc. London*, *Ser. A*, 1991, **335**, 365–375.
15. Klimm, K., Blundy, J. D. and Green, T. H., Trace element partitioning and accessory phase saturation during H_2O-saturated melting of basalt with implications for subduction zone chemical fluxes. *J. Petrol.*, 2008, **49**, 523–553.
16. Hermann, J. and Rubatto, D., Accessory phase control on the trace element signature of sediment melts in subduction zones. *Chem. Geol*., 2009, **265**, 512–526.
17. Arculus, R. J., The significance of source versus process in the tectonic controls of magma genesis. *J. Volcanol. Geotherm. Res*., 1987, **32**, 1–12.
18. Kelemen, P. B., Johnson, K. T. M., Kinzler, R. J. and Irving, A. J., High field strength element depletions in arc basalts due to mantle–magma interactions. *Nature*, 1990, **333**, 623–629.
19. McKenzie, D. and O'Nions, R. K., Partial melt distributions from the inversion of rare earth element concentrations. *J. Petrol.*, 1991, **32**, 1021–1091.
20. Thirlwall, M. F., Smith, T. E., Graham, A. M., Theodorou, N., Hollings, P., Davidson, J. P. and Arculus, R. J., High field strength element anomalies in arc lavas: source or process? *J. Petrol.*, 1994, **35**, 819–838.
21. Plank, T., Constraints from thorium/lanthanum on sediment recycling at subduction zones and the evolution of the continents. *J. Petrol.*, 2005, **46**, 921–944.
22. Weaver, B. L., The origin of ocean island basalt end-member compositions: trace and isotopic constraints. *Earth Planet. Sci. Lett*., 1991, **104**, 381–397.
23. Hofmann, A. W., Chemical differentiation of the earth: the relationship between mantle, continental crust, and oceanic crust. *Earth Planet. Sci. Lett.*, 1988, **90**, 297–314.
24. Fitton, J. G. and Dunlop, H. M., The Cameroon line, West Africa, and its bearing on the origin of oceanic and continental alkali basalt. *Earth Planet. Sci. Lett*., 1985, **72**, 23–38.
25. Wittke, J. H. and Mack, L. E., OIB-like mantle source for continental alkaline rocks of the Balcones province, Texas: trace-element and isotopic evidence. *J. Geol.*, 1993, **101**, 333–344.
26. Macdonald, R., Rogers, N. W., Fitton, J. G., Black, S. and Smith, M., Plume–lithosphere interactions in the generation of the basalts of the Kenya rift, East Africa. *J. Petrol.*, 2001, **42**, 877–900.
27. Späth, A., Le Roex, A. P. and Opiyo-Akech, N., Plume–lithosphere interaction and the origin of continental rift-related alkaline volcanism: the Chyulu Hills volcanic province, southern Kenya. *J. Petrol.*, 2001, **42**, 765–787.
28. Xu, Y. G., Ma, J. L., Frey, F. A., Feigenson, M. D. and Liu, J. F., Role of lithosphere–asthenosphere interaction in the genesis of Quaternary alkali and tholeiitic basalts from Datong, western North China Craton. *Chem. Geol*., 2005, **224**, 247–271.
29. Tang, Y. J., Zhang, H. F. and Ying, J. F., Asthenosphere–lithospheric mantle interaction in an extensional regime: implication from the geochemistry of Cenozoic basalts from Taihang Mountains, North China Craton. *Chem. Geol*., 2006, **233**, 309–327.
30. Latin, D., Norry, M. J. and Tarzey, R. J. E., Magmatism in the Gregory Rift, East Africa: evidence for melt generation by a plume. *J. Petrol.*, 1993, **34**, 1007–1027.
31. Goes, S., Spakman, H. and Bijwaard, H., A lower mantle source for Central European volcanism. *Science*, 1999, **286**, 1928–1931.
32. Wedepohl, K. H. and Baumann, A., Central European Cenozoic plume volcanism with OIB characteristics and indications of lower mantle source. *Contrib. Mineral. Petrol*., 1999, **136**, 225–239.
33. Johnson, J. S., Gibson, S. A., Thompson, R. N. and Nowell, G. M., Volcanism in the Vitim Volcanic Field, Siberia: geochemical evidence for a mantle plume beneath the Baikal rift zone. *J. Petrol.*, 2005, **46**, 1309–1344.
34. Altherr, R., Henjes-Kunst, F. and Baumann, A., Asthenosphere versus lithosphere as possible sources for basaltic magmas erupted during formation of the Red Sea: constraints from Sr, Pb and Nd isotopes. *Earth Planet. Sci. Lett*., 1990, **96**, 269–286.
35. Aldanmaz, E., Köprübaşi, N., Gürer, Ö. F., Kaymakçi, N. and Gourgaud, A., Geochemical constraints on the Cenozoic OIB-type alkaline volcanic rocks of NW Turkey: implications for mantle sources and melting processes. *Lithos*, 2006, **86**, 50–76.
36. Haase, K. M. and Devey, C. W., The petrology and geochemistry of Vesteris Seamount, Greenland basin – an intraplate alkaline volcano of non-plume origin. *J. Petrol.*, 1994, **35**, 295–328.
37. Wilson, M., Rosenbaum, J. M. and Dunworth, E. A., Melilitites: partial melts of the thermal boundary layer? *Contrib. Mineral. Petrol*, 1995, **119**, 181–196.
38. Thompson, R. N. *et al.*, Source of the Quaternary alkalic basalts, picrites and basanites of the Potrillo volcanic field, New Mexico, USA: lithosphere or convecting mantle? *J. Petrol.*, 2005, **46**, 1603–1643.
39. Hawkesworth, C. J., Kempton, P. D., Rogers, N. W., Ellam, R. M. and van Calstren, P., Continental mantle lithosphere and shallow level enrichment processes in the Earth's mantle. *Earth Planet. Sci. Lett*., 1990, **96**, 256–268.
40. Paslick, C., Halliday, A., James, D. and Dawson, J. B., Enrichment of the continental lithosphere by OIB melts: isotopic evidence from the volcanic province of northern Tanzania. *Earth Planet. Sci. Lett.*, 1995, **130**, 109–126.
41. Bedini, R. M., Bodinier, J.-L., Dautria, J.-M. and Morten, L., Evolution of LILE-enriched small melt fractions in the lithospheric mantle: a case study from the East African Rift. *Earth Planet. Sci. Lett*., 1997, **153**, 67–83.
42. Goodenough, K. M., Upton, B. G. J. and Ellam, R. M., Long-term memory of subduction processes in the lithospheric mantle: evidence from the geochemistry of basic dykes in the Gardar Province of South Greenland. *J. Geol. Soc. London*, 2002, **159**, 705–714.
43. Vijaya Kumar, K. and Leelanandam, C., Evolution of the Eastern Ghats Belt, India: a plate tectonic perspective. *J. Geol. Soc. India*, 2008, **72**, 720–749.
44. Dobmeier, C. J. and Raith, M. M., Crustal architecture evolution of the Eastern Ghats Belt and adjacent regions of India. In *Proterozoic East Gondwana: Supercontinent Assembly and Breakup* (eds Yoshida, M., Windley, B. F. and Dasgupta, S.), Geological Society of London, Spl. Publ., 2003, vol. 206, pp. 145–168.

45. Vijaya Kumar, K. and Leelanandam, C., Crustal growth in magmatic arcs: the Kondapalli arc, Eastern Ghats Belt, India. In National Seminar on 'Active and Fossil Suture Zones', Dehra Dun, abstr., 2006, pp. 119–120.
46. Leelanandam, C. and Vijaya Kumar, K., Petrogenesis and tectonic setting of the chromitites and chromite-bearing ultramafic cumulates of the Kondapalli Layered Complex, Eastern Ghats Belt, India: evidences from the textural, mineral–chemical and whole-rock geochemical studies. In *Indian Continental Crust and Upper Mantle* (eds Leelanandam, C. *et al.*), IAGR Memoir. 10 (in honour of T. M. Mahadevan), 2007, pp. 89–107.
47. Vijaya Kumar, K., Leelanandam, C. and Ernst, W. G., Formation and fragmentation of the Paleoproterozoic supercontinent Columbia: evidence from the Eastern Ghats Granulite Belt, SE India. *Int. Geol. Rev.*, 2011, **53**, 1297–1311.
48. Dharma Rao, C. V. and Santosh, M., Continental arc magmatism in a Mesoproterozoic convergent margin: petrological and geochemical constraints from the magmatic suite of Kondapalle along the eastern margin of the Indian plate. *Tectonophysics*, 2011, **510**, 151–171.
49. Kovach, V. P. *et al.*, The western charnockite zone of the Eastern Ghats Belt, India: an independent crustal province of late Archean (2.8 Ga) and Paleoproterozoic (1.7–1.6 Ga) terrains. *Gondwana Res*., 2001, **4**, 666–667.
50. Bose, S., Dunkley, D. J., Dasgupta, S., Das, K. and Arima, M., India–Antarctica–Australia–Laurentia connection in the Paleoproterozoic–Mesoproterozoic revisited: evidence from new zircon U–Pb and monazite chemical age data from the Eastern Ghats Belt, India. *GSA Bull.*, 2011, **123**, 2031–2249.
51. Vijaya Kumar, K., Ernst, W. G., Leelanandam, C., Wooden, J. L. and Grove, M. J., Geochronologic–geochemical documentation of a Paleoproterozoic suprasubduction-zone ophiolite from Kandra, SE India. *Tectonophysics*, 2010, **487**, 22–32.
52. Mezger, K. and Cosca, M. A., The thermal history of the Eastern Ghats Belt (India) as revealed by U–Pb and $^{40}Ar/^{39}Ar$ dating of metamorphic and magmatic minerals: implications for the SWEAT correlation. *Precambrian Res.*, 1999, **94**, 251–271.
53. Simmat, R. and Raith, M. M., U–Th–Pb monazite geochronometry of the Eastern Ghats Belt, India: timing and spatial disposition of poly-metamorphism. *Precambrian Res.*, 2008, **162**, 16–39.
54. Upadhyay, D., Gerdes, A. and Raith, M. M., Unraveling sedimentary provenance and tectonothermal history of high to ultrahigh temperature metapelites using zircon and monazite chemistry: a case study from the Eastern Ghats Belt, India. *J. Geol.*, 2009, **117**, 665–683.
55. Henderson, B., Collins, A. S., Payne, J., Forbes, C. and Saha, D., Geologically constraining India in Columbia: the age, isotopic provenance and geochemistry of the protoliths of the Ongole domain, southern Eastern Ghats, India. *Gondawana Res*., 2013; doi:10.1016/j.gr.2013.09.002.
56. Leelanandam, C., The Kondapalli layered complex, Andhra Pradesh, India: a synoptic overview. *Gondwana Res*., 1997, **1**, 95–114.
57. Leelanandam, C., The Kandra volcanics in Andhra Pradesh: possible ophiolite? *Curr. Sci.*, 1990, **59**, 785–788.
58. Sesha Sai, V. V., Sheeted dykes in Kandra ophiolite complex, Nellore Schist Belt, Andhra Pradesh – vestiges of Precambrian oceanic crust. *J. Geol. Soc. India*, 2009, **74**, 509–514.
59. Saha, D., Dismembered ophiolites in Paleoproterozoic nappe complexes of Kandra and Gurramkonda, South India. *J. Asian Earth Sci*., 2011, **42**, 158–175.
60. Ravikant, V., Palaeoproterozoic (~ 1.9 Ga) extension and breakup along the eastern margin of the Eastern Dharwar Craton, SE India: new Sm–Nd isochron age constraints from an orogenic mafic magmatism in the Neoarchean Nellore greenstone belt. *J. Asian Earth Sci*., 2010, **37**, 67–81.
61. Sarkar, A. and Paul, D. K., Geochronology of the Eastern Ghats Precambrian mobile belt – a review. *Geol. Surv. India*, *Spec. Publ*., 1998, **44**, 51–86.
62. Upadhyay, D., Raith, M. M., Mezger, K. and Hammerschmidt, K., Mesoproterozoic rift-related alkaline magmatism at Elchuru, Prakasam Alkaline Province, SE India. *Lithos*, 2006, **89**, 447–477.
63. Vijaya Kumar, K., Frost, C. D., Frost, B. R. and Chamberlain, R., The Chimakurti, Errakonda, and Uppalapadu plutons, Eastern Ghats Belt, India: an unusual association of tholeiitic and alkaline magmatism. *Lithos*, 2007, **97**, 30–57.
64. Vijaya Kumar, K., Ernst, W. G. and Leelanandam, C., Opening and closing of a Mesoproterozoic Ocean along the SE margin of India: textural, cathodoluminescence and SHRIMP analyses of zircon. In American Geophysical Union Fall Meeting, San Francisco, abstr. V14B–07, 2011.
65. Subba Rao, T. V., Bhaskar Rao, Y. J., Sivaraman, T. V. and Gopalan, K., Rb–Sr age and petrology of the Elchuru alkaline complex: implications to alkaline magmatism in the Eastern Ghat Mobile Belt. In *Alkaline Rocks* (ed. Leelanandam, C.), Memoir Geological Society of India, 1989, vol. 15, pp. 207–223.
66. Rathna, K., Vijaya Kumar, K. and Ratnakar, J., Petrology of the dykes of Ravipadu, Prakasam Province, Andhra Pradesh, India. *J. Geol. Soc. India*, 2000, **55**, 399–412.
67. Vijaya Kumar, K. and Rathna, K., Geochemistry of the mafic dykes in the Prakasam Alkaline Province of Eastern Ghats Belt, India: implications for the genesis of continental rift zone magmatism. *Lithos*, 2008, **104**, 306–326.
68. Pearce, J. A. and Cann, J. R., Ophiolite origin investigated by discriminant analysis using Ti, Zr and Y. *Earth Planet. Sci. Lett*., 1971, **12**, 290–349.
69. Wood, D. A., Joron, J.-L. and Treuil, M., A re-appraisal of the use of trace elements to classify and discriminate between magma series erupted in different tectonic setting. *Earth Planet. Sci. Lett*., 1979, **50**, 11–30.
70. Pearce, J. A. and Peate, D. W., Tectonic implications of the composition of volcanic arc magmas. *Annu. Rev. Earth Planet. Sci*., 1995, **23**, 251–285.
71. Pearce, J. A., Geochemical fingerprinting of oceanic basalts with applications to ophiolite classification and the search for Archean oceanic crust. *Lithos*, 2008, **100**, 14–48.
72. Fitton, J. G., Saunders, A. D., Norry, M. J., Hardarson, B. S. and Taylor, R. N., Thermal and chemical structure of the Iceland plume. *Earth Planet. Sci. Lett*., 1997, **153**, 197–208.
73. Condie, K. C., High field strength element ratios in Archean basalts: a window to evolving sources of mantle plumes? *Lithos*, 2005, **79**, 491–504.
74. Gao, S., Luo, T.-C., Zhang, B.-R., Zhang, H.-F., Han, Y.-W., Zhao, Z.-D. and Hu, Y.-K., Chemical composition of the continental crust as revealed by studies in east China. *Geochim. Cosmochim. Acta*, 1998, **62**, 1959–1975.
75. Plank, T. and Langmuir, C. H., The chemical composition of subducting sediment and its consequences for the crust and mantle. *Chem. Geol.*, 1998, **145**, 325–394.
76. Barth, M. G., McDonough, W. F. and Rudnick, R. L., Tracking the budget of Nb and Ta in the continental crust. *Chem. Geol*., 2000, **165**, 197–213.
77. Crawford, A. J., Falloon, T. J. and Eggins, S., The origin of island arc high-alumina basalts. *Contrib. Mineral. Petrol*., 1987, **97**, 417–430.
78. Gaetani, G. and Grove, T. L., The influence of water on melting of mantle peridotite. *Contrib. Mineral. Petrol*., 1998, **131**, 323–346.
79. Canil, D., Vanadium in peridotites, mantle redox and tectonic environments: Archean to present. *Earth Planet. Sci. Lett*., 2002, **195**, 75–90.
80. Hanson, G. N., Rare earth elements in petrogenetic studies of igneous systems. *Annu. Rev. Earth Planet. Sci*., 1980, **8**, 371–406.

81. Kay, R. W., Volcanic arc magmas: implication of a melting–mixing model for element recycling in the crust–upper mantle system. *J. Geol.*, 1980, **88**, 497–522.
82. Armstrong, R. L., Radiogenic isotopes: the case for crustal recycling on a near-steady-state no-continental-growth earth. *Philos. Trans. R. Soc. London*, 1981, **301**, 443–472.
83. Plank, T. and Langmuir, C. H., Tracing trace elements from sediment input to volcanic output at subduction zones. *Nature*, 1993, **362**, 739–743.
84. Pearce, J. A., Supra-subduction zone ophiolites: the search for modern analogues. *Geol. Soc. Am. Spec. Pap.*, 2003, **373**, 269–293.
85. Ringwood, A. E., The petrological evolution of island arc system. *J. Geol. Soc. London*, 1974, **130**, 183–204.
86. Spandler, C. and Pirard, C., Element recycling from subducting slabs to arc crust: a review. *Lithos*, 2013, **170–171**, 208–223.
87. Sun, S.-S. and McDonough, W. F., Chemical and isotopic systematics of oceanic basalts: implications for mantle composition and processes. In *Magmatism in the Ocean Basins* (eds Saunders, A. D. and Norry, M. J.), Geological Society Spl. Publ., 1989, vol. 42, pp. 313–345.
88. Shaw, D. M., Trace element fractionation during anatexis. *Geochim. Cosmochim. Acta*, 1970, **34**, 237–243.
89. Saunders, A. D., Tarney, J. and Weaver, S. D., Traverse geochemical variations across the Antarctica peninsula: implications for the genesis of calc-alkaline magmas. *Earth Planet. Sci. Lett.*, 1980, **46**, 344–360.
90. Ryerson, F. J. and Watson, E. B., Rutile saturation in magmas: implications for Ti–Nb–Ta depletion in island-arc basalts. *Earth Planet. Sci. Lett.*, 1987, **86**, 225–239.
91. Kelemen, P. B., Shimizu, N. and Dunn, T., Relative depletion of Nb in some arc magmas and the continental crust: partitioning of K, Nb, La and Ce during melt/rock reaction in the upper mantle. *Earth Planet. Sci. Lett.*, 1993, **120**, 111–133.
92. Elliot, T., Plank, T., Zindler, A., White, W. and Bourdon, B., Element transport from slab to volcanic front at the Mariana arc. *J. Geophys. Res.*, 1997, **102**, 14,991–15,019.
93. Ewart, A. and Hawkesworth, C. J., The Pleistocene–Recent Tonga–Kermadec arc lavas: interpretation of new isotopic and rare earth data in terms of a depleted mantle source. *J. Petrol.*, 1987, **28**, 495–530.
94. Salters, V. J. and Shimizu, N., World-wide occurrence of HFSE-depleted mantle. *Geochim. Cosmochim. Acta*, 1988, **52**, 2177–2182.
95. Woodhead, J., Eggins, S. and Gamble, J., High field strength and transition element systematic in island arc and back-arc basin basalts; evidence for multi-phase melt extraction and a depleted mantle wedge. *Earth Planet. Sci. Lett.*, 1993, **114**, 491–504.
96. Hofmann, A. W. and White, W. M., Mantle plumes from ancient oceanic crust. *Earth Planet. Sci. Lett.*, 1982, **57**, 421–436.
97. McKenzie, D. and O'Nions, R. K., The source regions of ocean island basalts. *J. Petrol.*, 1995, **36**, 133–159.
98. Class, C., Miller, D. M., Goldstein, S. L. and Langmuir, H., Distinguishing melt and fluid subduction components in Umnak volcanic, Aleutian arc. *Geochem. Geophys. Geosyst.*, 2000, **1**, 1999GC000010.
99. Spandler, C., Mavrogenes, J. and Hermann, J., Experimental constraints on element mobility from subducted sediments using high-P synthetic fluid/melt inclusions. *Chem. Geol.*, 2007, **239**, 228–249.
100. Ratnakar, J., Vijaya Kumar, K. and Rathna, K., A geochemical analysis of the alkaline mafic dykes in the environs of the Prakasam Alkaline Province, Eastern Ghats Belt, India. In *Indian Dykes* (eds Srivatsava, R. K., Chalapati Rao, N. V. and Ch. Sivaji), Narosa Publications, New Delhi, 2008, pp. 291–308.
101. Vijaya Kumar, K., Ernst, W. G. and Leelanandam, C., Geochronologic and tectonic evolution of the Eastern Ghats Belt, India. *DST-DCS News Lett.*, 2013, pp. 10–15.
102. Weaver, S. D., Saunders, A. D., Pankhurst, R. J. and Tarney, J., A geochemical study of magmatism associated with the initial stages of back-arc spreading. *Contrib. Mineral. Petrol*, 1979, **68**, 151–169.
103. Cousens, B. L., Allan, J. F. and Corton, M. P., Subduction-modified pelagic sediments as the enriched component in back-arc basalts from the Japan Sea: ocean drilling program sites 797 and 794. *Contrib. Mineral. Petrol.*, 1994, **117**, 421–434.
104. Dudás, F. Ö., Geochemistry of igneous rocks from the Crazy Mountains, Montana, and tectonic models for the Montana alkalic province. *J. Geophys. Res.*, 1991, **96**, 13261–13277.
105. Wang, Y. J., Fan, W. M., Zhang, H. F. and Peng, T. P., Early Cretaceous gabbroic rocks from the Taihang Mountains: implications for a paleosubduction-related lithospheric mantle beneath the central North China Craton. *Lithos*, 2006, **86**, 281–302.
106. Dharma Rao, C. V., Santosh, M. and Dong, Y., U–Pb zircon chronology of the Pangidi–Kondapalle layered intrusion, Eastern Ghats belt, India: constraints on Mesoproterozoic arc magmatism in a convergent margin setting. *J. Asian Earth Sci.*, 2012, **49**, 362–375.
107. Johnson, R. W., Mackenzie, D. E. and Smith, I. E. M., Delayed partial melting of subduction-modified mantle in Papua New Guinea. *Tectonophysics*, 1978, **46**, 197–216.
108. Rudnick, R. L., Making continental crust. *Nature*, 1995, **378**, 571–578.
109. Shaw, D. M., Continuous (dynamic) melting theory revisited. *Can. Mineral.*, 2000, **38**, 1041–1063.
110. Adam, J. and Green, T., Trace element partitioning between mica- and amphibole-bearing garnet lherzolite and hydrous basanitic melt: 1. Experimental results and the investigation of controls on partitioning behavior. *Contrib. Mineral. Petrol.*, 2006, **152**, 1–17.
111. Workman, R. K. and Hart, S. R., Major and trace element composition of the depleted MORB mantle (DMM). *Earth Planet. Sci. Lett.*, 2005, **231**, 53–72.

ACKNOWLEDGEMENTS. We thank Prof. V. Rajamani for inviting us to contribute an article to this special section. K.V.K. and K.R. have hugely benefited by discussions with Prof. Rajamani over the years on the principles of geochemistry. We appreciate funding from CSIR (Emeritus Scientist Scheme to C.L.), DST (ESS/16/165/2002 and BOYSCAST Fellowship to K.V.K.), IUSSTF (Research Fellowship to K.V.K.) and UGC (post-doctoral fellowship to K.R.) over the years for our research on the Eastern Ghats Belt. We thank Prof. Gary Ernst (Stanford University, USA) and Sri T. M. Mahadevan (Former Director, Atomic Minerals Division) for constructive and helpful comments on an earlier version of the manuscript.